Implementation of umbrella integration within the framework of the empirical valence bond approach

Dhruva K. Chakravorty, **Malika Kumarasiri**, **Alexander V. Soudackov**, and **Sharon Hammes-Schiffer**

Department of Chemistry, 104 Chemistry Building, Pennsylvania State University, University Park, PA 16802; e-mail: shs@chem.psu.edu

Abstract

The umbrella integration method for calculating the potential of mean force (PMF) for a chemical reaction is implemented within the empirical valence bond (EVB) framework. In this implementation, the PMF is generated along the energy gap reaction coordinate, and the biasing potential is the difference between the mapping potential, which is defined to be a linear combination of the valence bond state energies, and the EVB ground state energy. The umbrella integration method is based on the derivative of the PMF with respect to the reaction coordinate. An analytical expression for this derivative applicable to certain types of EVB potentials is presented. The advantages of the umbrella integration method are illustrated by the application of both umbrella integration and the weighted histogram analysis method to the hydride transfer reaction catalyzed by the enzyme dihydrofolate reductase. This application demonstrates that the umbrella integration method reduces the statistical errors, converges efficiently, and does not require significantly overlapping windows. A modified version of the weighted histogram analysis method that shares these advantages is also proposed and implemented.

I. Introduction

The calculation of free energy barriers for chemical reactions is critical for predicting reaction rates. The free energy barrier is typically obtained by generating the potential of mean force (PMF) along a specified reaction coordinate. In umbrella sampling,[1] the PMF is generated by performing molecular dynamics or Monte Carlo simulations with a series of biasing potentials that enable sampling of the entire relevant range of the reaction coordinate. The probability distribution along the reaction coordinate for each biasing potential is obtained using standard binning techniques. Various methods have been developed for combining the probability distributions for the different biasing potentials to obtain the complete PMF for the unbiased system. The weighted histogram analysis method (WHAM) has been used extensively for this purpose.[2-7] Recently, Kästner and Thiel presented the alternative umbrella integration (UI) method.[8, 9] The advantages of the UI method are that it avoids the iterative procedure inherent to WHAM, reduces the statistical errors, and converges more efficiently.[8, 9] The previous implementation of UI considered only biasing potentials in the form of harmonic restraints along the reaction coordinate.[8, 9]

In this paper, we implement UI within the framework of the empirical valence bond (EVB) approach, in conjunction with an energy gap reaction coordinate and non-harmonic biasing potentials defined in terms of mapping potentials. The empirical valence bond (EVB) approach has been used successfully to describe a wide range of chemical reactions in solution and proteins.[10-14] In this approach, the chemical reaction is described in terms of a small number of valence bond states, and the EVB electronic ground state is obtained by diagonalizing the Hamiltonian matrix formed in the basis of these VB states. Single proton, hydride, and electron

transfer reactions are often described in terms of two valence bond states, and the energy gap reaction coordinate is defined to be the difference between the energies of these two valence bond states. When umbrella sampling is used to generate the PMF along the energy gap reaction coordinate, the biasing potential may be chosen to be the energy difference between a mapping potential, which is a linear combination of the energies of the two valence bond states, and the EVB electronic ground state energy. Previously, we used thermodynamic integration and WHAM to generate the PMF within the framework of this EVB approach for charge transfer reactions in enzymes.[15-18] We also proposed and utilized an approach for calculating the rate constant from this PMF.[19] The implementation of UI within this framework provides an alternative method with the advantages enumerated above.

An outline of the paper is as follows. In Section II, we summarize the WHAM and UI approaches and present the equations required for the implementation of UI within the framework of the EVB approach. In Section III, we use both WHAM and UI to generate the PMF for the hydride transfer reaction catalyzed by the enzyme dihydrofolate reductase (DHFR). Our analysis of these calculations illustrates the advantages of UI over WHAM for this type of system. We also propose and implement a modification to WHAM that leads to similar advantages. The conclusions are presented in Section IV.

II. Methods

In umbrella sampling,[1] simulations are performed with a series of biasing potentials $w_i(\xi)$, where ξ is the reaction coordinate. The distribution $P_i^b(\xi)$ of the biased system along the reaction coordinate is typically obtained by standard binning procedures to generate a histogram. Specifically, the relevant range of the reaction coordinate is divided into bins, and $P_i^b(\xi_{bin})$ is the fraction of sampled configurations in the bin centered at the reaction coordinate ξ_{bin} for the window corresponding to the biasing potential $w_i(\xi)$. The PMF for the biased system along the reaction coordinate is given by:

$$A_i^b(\xi) = -\frac{1}{\beta}\ln \quad P_i^b(\xi),$$

(1)

where $\beta = 1/k_B T$. The PMF for the unbiased system in each window is

$$A_i^u(\xi) = -\frac{1}{\beta}\ln \quad P_i^b(\xi) - w_i(\xi) + F_i,$$

(2)

where F_i are constants that differ for each biasing potential or window.

In WHAM,[2-6] the constants F_i are calculated iteratively to combine the unbiased potentials of mean force for different windows. The following two equations are solved iteratively:

$$P(\xi) = \sum_i^{windows} N_i P_i^b(\xi) / \sum_j^{windows} N_j e^{[F_j - w_j(\xi)]\beta}$$

(3)

$$e^{-F_i\beta} = \int d\xi e^{-w_i(\xi)\beta} P(\xi)$$

(4)

where N_i is the total number of configurations sampled for window i used to construct $P_i^b(\xi)$. After these equations are solved to self consistency, the PMF $A(\xi)$ is obtained directly from $P(\xi)$ using the relation $A(\xi) = -\ln P(\xi)/\beta$.

In UI,[8, 9] the derivative of the unbiased PMF with respect to the reaction coordinate is calculated for each window:

$$\frac{\partial A_i^u(\xi)}{\partial \xi} = -\frac{1}{\beta}\frac{\partial \ln P_i^b(\xi)}{\partial \xi} - \frac{dw_i(\xi)}{d\xi}.$$

(5)

The data from different windows are combined according to a weighted average:

$$\frac{\partial A(\xi)}{\partial \xi} = \sum_i^{windows} p_i(\xi)\left(\frac{\partial A_i^u(\xi)}{\partial \xi}\right)$$

(6)

where

$$p_i(\xi) = N_i P_i^b(\xi) / \sum_i N_i P_i^b(\xi).$$

(7)

Subsequently, $A(\xi)$ is obtained by numerical integration over ξ. In previous applications of UI, the biasing potential is assumed to be of the form $w_i(\xi) = K(\xi - \xi_i)^2/2$. Moreover, the biased PMF is expanded in a power series and truncated after the quadratic term, which is equivalent to assuming a normal distribution for $P_i^b(\xi)$:

$$P_i^b(\xi) = \frac{1}{\sigma_i^b \sqrt{2\pi}} \exp\left[-\frac{1}{2}\left(\frac{\xi - \bar{\xi}_i^b}{\sigma_i^b}\right)^2\right],$$

(8)

where the mean $\bar{\xi}_i^b$ and the variance σ_i^b for each window are determined from the simulation data. These approximations lead to an analytical expression for the derivative of the unbiased PMF given in Eq. 5.

The UI method differs from WHAM in two important aspects. First, the UI method is based on the derivative of the PMF, rather than the PMF itself, so it does not involve offsets and therefore avoids the iterative procedure inherent to WHAM. Second, UI does not require a binning procedure because the mean and variance of the normal distribution for each window are determined directly from the raw simulation data, so a binning procedure is not required to obtain the derivative of the PMF given in Eq. 6. Specifically, the values of the reaction coordinate for all configurations sampled are collected during the simulation, and the mean and variance of the reaction coordinates collected for each window are determined directly from these data without generating a histogram. Moreover, in our implementation, the numerical integration of this derivative to generate the PMF is performed using an adaptive integration method that is converged to a specified precision without requiring the specification of a bin width. These numerical integrals are evaluated using the global adaptive strategy[20] in conjunction with the Gauss-Kronrod quadrature rule[21] as implemented in the Mathematica software package.[22]

To facilitate a meaningful comparison of the WHAM and UI methods, we propose a modified version of the WHAM method, denoted WHAM(n), that also avoids the binning procedure. In WHAM(n), the biased distribution $P_i^{\rm b}(\xi)$ for each window is represented by the normal distribution given in Eq. 8, where the mean and variance of ξ for each window are determined directly from the simulation data. The WHAM equations given in Eqs. 3 and 4 are still solved iteratively, but $P_i^{\rm b}(\xi)$ in Eq. 3 is represented by the analytical normal distribution rather than the histogram obtained from a binning procedure. The integration in Eq. 4 is performed numerically using the adaptive integration method discussed above, thereby eliminating the necessity of specifying a bin width. Statistical methods[23] may be used to determine the error bars for the mean and variance of ξ used in Eq. 8 for both UI and WHAM(n). In addition to these statistical errors, a truncation error is introduced for both of these methods due to the approximation of the biased distribution by a normal distribution. A detailed analysis of the different sampling errors associated with UI has been performed for an analytical model potential.[9]

The main objective of this paper is to implement the UI method within the framework of a two-state EVB potential using an energy gap reaction coordinate and a mapping potential. For a two-state EVB model, the ground state EVB energy is

$$V_{\rm EVB} = \frac{1}{2}\,(V_{11}+V_{22}) - \frac{1}{2}\,\sqrt{(V_{11}-V_{22})^2+4V_{12}^2}$$

(9)

where V_{11} and V_{22} are the energies of VB states 1 and 2, respectively, and V_{12} is the coupling between these two states. In general, all of these quantities depend on the nuclear coordinates of the system. The energy gap reaction coordinate is defined as $\xi=V_{11}-V_{22}$. The simulations are performed with mapping potentials

$$V_{\rm map}^i = (1-\lambda_i)\,V_{11}+\lambda_i V_{22},$$

(10)

where the mapping parameter λ_i is varied from zero to unity. The biasing potential is then of the form

$$w_i(\xi) = V_{\rm map}^i - V_{\rm EVB} = \left(\frac{1}{2}-\lambda_i\right)\xi + \frac{1}{2}\,\sqrt{\xi^2+4V_{12}^2}.$$

(11)

Note that this biasing potential is a function of only ξ if V_{12} is a function of only ξ. In this paper, we assume that V_{12} is a constant, although the extension to the case in which V_{12} is a function of ξ is straightforward. Using this form for the biasing potential, the derivative of the unbiased PMF given in Eq. 5 is expressed as

$$\frac{\partial A_i^{\rm u}}{\partial \xi} = -\frac{1}{\beta}\frac{\partial \ln P_i^{\rm b}(\xi)}{\partial \xi} - \left(\frac{1}{2}-\lambda_i+\frac{\xi}{2\sqrt{\xi^2+4V_{12}^2}}\right).$$

(12)

Approximating $P_i^{\rm b}(\xi)$ by a normal distribution, we have obtained an analytical form for the derivative of the unbiased PMF for each window. The data for the different windows can be combined using Eq. 6, followed by numerical integration of the derivative of the PMF over ξ to obtain the PMF $A(\xi)$.

We also explore the use of different forms for the biased distribution $P_i^b(\xi)$ because the mapping potential could lead to deviations from a normal distribution. We present results for the Gram-Charlier and the asymptotic Edgeworth expansions, which are expansions in terms of Chebyshev-Hermite polynomials. The Gram-Charlier expansion is of the form[24]

$$P_i^b(\xi) = \frac{1}{\sigma_i^b \sqrt{2\pi}} \exp\left[-\frac{1}{2}\left(\frac{\xi - \bar{\xi}_i^b}{\sigma_i^b}\right)^2\right]$$
$$\times \left[1 + \frac{\kappa_3}{3!(\sigma_i^b)^5} He_3\left(\frac{\xi - \bar{\xi}_i^b}{\sigma_i^b}\right) + \frac{\kappa_4}{4!(\sigma_i^b)^6} He_4\left(\frac{\xi - \bar{\xi}_i^b}{\sigma_i^b}\right) + \frac{10}{6!}\left(\frac{\kappa_3}{(\sigma_i^b)^5}\right)^2 He_6\left(\frac{\xi - \bar{\xi}_i^b}{\sigma_i^b}\right) + \dots\right]$$

(13)

where

$$He_n(x) = (-1)^n e^{x^2/2} \frac{d^n}{dx^n} e^{-x^2/2}$$

are Chebyshev-Hermite polynomials, σ_i^b is the variance, and κ_n are the cumulants of the distribution $P_i^b(\xi)$. The asymptotic Edgeworth expansion can be presented in the following compact form[25]

$$P_i^b(\xi) = \frac{1}{\sigma_i^b \sqrt{2\pi}} \exp\left[-\frac{1}{2}\left(\frac{\xi - \bar{\xi}_i^b}{\sigma_i^b}\right)^2\right] \left\{1 + \sum_{s=1}^{\infty}(\sigma_i^b)^s \times \sum_{\{k_m\}} He_{s+2r}(x) \prod_{m=1}^{s} \frac{1}{k_m!}\left(\frac{S_{m+2}}{(m+2)!}\right)^{k_m}\right\},$$

(14)

where $S_n \equiv \kappa_n/(\sigma_i^b)^{2n-2}$, $\{k_m\}$ are the solutions of the Diophantine equation $k_1 + 2k_2 + \dots + sk_s = s$, and $r = k_1 + k_2 + \dots + k_s$. These asymptotic expansions are useful when the biased distributions for some windows differ from the normal distributions. The derivatives of the asymptotic expansions can still be evaluated analytically, and the moments and cumulants of the biased distributions can be calculated directly from the raw sampling data.

III. Application

We use both WHAM and UI to calculate the PMF for hydride transfer in the enzyme DHFR. In this reaction, the hydride is transferred from the NC4 position of the NADPH (nicotinamide adenine dinucleotide phosphate) cofactor to the C6 position of the protonated dihydrofolate substrate. This reaction is depicted in Figure 1. We studied this reaction previously with a hybrid quantum-classical molecular dynamics approach, which includes the nuclear quantum effects of the transferring hydrogen with grid-based or path integral methods.[16-18] Here we use the same simulation system and EVB potential but do not include the nuclear quantum effects for simplicity. Since the simulations details are given elsewhere,[16, 17] we provide only a brief summary in the present paper.

The simulation system includes the entire protein, the substrate, and the cofactor solvated by 4122 explicit water molecules in a truncated octahedral periodic box. The initial coordinates were obtained from a crystal structure of *Escherichia coli* DHFR complexed with NADP$^+$ and folate (PDB code 1rx2).[26] The potential energy surface is represented by a two-state EVB potential,[10] where state 1 corresponds to the transferring hydrogen atom bonded to the donor, and state 2 corresponds to the transferring hydrogen atom bonded to the acceptor. The diagonal elements of the EVB Hamiltonian are based on the GROMOS force field[27] with the EVB

parameters given in Ref. 17. The two EVB parameters corresponding to the relative energy of the two valence bond states and the coupling between these states were fit to the experimental free energies of reaction and activation.[28]

In previous simulations, we used a set of 20 mapping parameters and performed 4.5 ns of molecular dynamics for each window with an additional 2 ns for the four windows near the transition state.[17] For the analysis in the present paper, we generated new data, starting with a snapshot from a reactant window in the previous simulation. We used a set of 19 mapping parameters from $\lambda_i = 0.05$ to 0.95 with a spacing of 0.05. The starting configuration for each window was obtained from the previous window after 20 ps of equilibration. Each window was equilibrated for a total of 350 ps, followed by 300 ps of data collection. We also generated two other independent sets of data with 50 ps of equilibration followed by 300 ps of data collection. The free energy barriers determined from these three data sets, as well as the previous simulations,[17, 18] differ by less than 0.5 kcal/mol.

Figure 2 illustrates that the PMF curves generated with UI and WHAM are very similar. The free energy barriers of 15.0 kcal/mol and 15.3 kcal/mol determined with UI and WHAM, respectively, are consistent with the classical barriers determined from previous simulations using both thermodynamic integration and WHAM. However, the WHAM curve exhibits more numerical noise, particularly in the reactant and product wells. The WHAM curve in Figure 2 was generated with a bin size of 1 kcal/mol. The impact of bin size on the systematic and statistical errors in WHAM has been discussed in the literature.[29]

As discussed above, an advantage of UI is that it does not require a binning procedure for the simulation data, although it does require numerical integration to generate the PMF from its derivative. In contrast, WHAM relies on a binning procedure to generate the biased distributions used in the iterative procedure to determine the overall unbiased distribution. Moreover, WHAM does not converge as the number of bins increases (i.e., as the bin width decreases) because the statistical error increases as the number of bins increases.[29] In particular, the bin width must be sufficiently large to ensure that a sufficient number of configurations are sampled for each bin. Insufficient sampling per bin leads to large statistical fluctuations that can result in substantial inaccuracies in the probability densities generated with WHAM. These difficulties with statistical error are avoided in UI because the biased distribution is represented by the analytical normal distribution function given in Eq. 8, where the mean and variance of the reaction coordinate for each window are obtained directly from the simulation data. In addition, a low weight is assigned to the tails of the distribution from each window in UI, as indicated by Eq. 7. As mentioned above, statistical methods[23] may be used to provide well-defined error bars for the mean and variance of the reaction coordinate, which can be propagated to estimate the sampling error for the resulting PMF.

Figure 3a illustrates the impact of bin size on the PMF curve generated with WHAM. Decreasing the bin size from 1.0 kcal/mol to 0.2 kcal/mol significantly increases the statistical noise of the PMF generated with WHAM. For comparison, Figure 3b depicts the PMF curve generated with the WHAM(n) method. This figure indicates that the statistical errors in WHAM are significantly reduced when the biased distribution for each window is represented by the analytical normal distribution function rather than the histogram obtained from the binning procedure. This figure also illustrates that the PMF curve generated with WHAM(n) is virtually indistinguishable from the PMF curve generated with UI.

Another advantage of UI is that it does not require overlap between the distributions of the windows, although such overlap is desirable to enhance the accuracy. In contrast, WHAM requires sufficient overlap between the distributions of the windows. Figure 4 depicts the PMF generated with UI, WHAM, and WHAM(n) using only five windows corresponding to $\lambda_i =$

0.05, 0.15, 0.50, 0.85, and 0.95 (i.e., two windows in the reactant and product regions and one window in the barrier region). The PMF curve generated with UI using only five windows is virtually identical to the curve generated with all 19 windows. In contrast, the PMF curve generated with WHAM using only five windows is clearly problematic, as illustrated by Fig. 4b. The barrier improves as the convergence criterion for the constants F_i determined during the iterative procedure is tightened from a maximum change of 10^{-4} to 10^{-8}, but the number of iterations required for convergence increases to more than 7.6×10^7 for a convergence criterion of 10^{-8}, which still does not generate a smooth PMF. As shown in Fig. 4c, the PMF curve generated with WHAM(n) using only five windows is better than that generated with WHAM for the same convergence criterion, but WHAM(n) still requires more than 8.6×10^4 iterations for a convergence criterion of 10^{-6}, which generates a PMF that is indistinguishable from the PMF generated with WHAM(n) using all 19 windows.

In principle, given sufficient sampling within each window, WHAM and UI should converge to the same results if the distributions are Gaussian. However, the convergence of the iterative procedure in WHAM becomes slow for small overlap between the distributions of the windows, and insufficient sampling of the tail regions of the distributions combined with very small overlap could preclude convergence. An advantage of UI is that it utilizes an analytical expression for the distributions, thereby decreasing the statistical noise. Moreover, UI does not require an iterative procedure, so convergence is not an issue. These advantages become particularly pronounced for small overlaps between the distributions of the windows, although additional windows will enhance the accuracy of both methods.

Lastly, we test the approximation of the biased distribution function $P_i^b(\xi)$ by a normal distribution, as given in Eq. 8. For this purpose, we explore the use of the Gram-Charlier and Edgeworth expansions.[25] The data and biased distribution functions for a representative window in the reactant region are shown in Figure 5a. The Gram-Charlier expansion is virtually indistinguishable from the normal distribution, whereas the Edgeworth expansion slightly improves the fit of the distribution obtained from the simulation data. As shown in Figure 5b, however, all three distribution functions lead to indistinguishable PMF curves. These data indicate that the approximation of the biased distribution by a normal distribution function is sufficient for generating quantitatively accurate PMF curves for this system. Note that this approximation may not be valid for certain systems, particularly when weak biasing potentials are used for free energy surfaces with high barriers or extended flat regions. In these cases, the WHAM method based on histograms obtained from a binning procedure could be more effective than the UI method.

IV. Conclusions

In this paper, we implemented the UI method for calculating the PMF along an energy gap reaction coordinate within the EVB framework. The UI method is based on the derivative of the PMF with respect to the reaction coordinate rather than the PMF itself. In this implementation, the biasing potential is the difference between the mapping potential, which is defined to be a linear combination of the valence bond state energies, and the EVB ground state energy. This biasing potential can be expressed as an analytical function of the energy gap reaction coordinate for a two-state EVB model in which the coupling between the two states is constant or is a function of the reaction coordinate. In this case, the derivative of the biasing potential with respect to the reaction coordinate can be expressed analytically, and the implementation of the UI method is straightforward.

We applied the UI and WHAM methods to the hydride transfer reaction catalyzed by DHFR. We showed that the UI and WHAM methods generate very similar PMF curves, although the PMF curve generated with UI exhibited less statistical noise. We also showed that the

representation of the biased probability distributions as normal distributions is reasonable by comparison to expansions including non-Gaussian effects. Furthermore, our analysis illustrated two significant advantages of UI over WHAM. The first advantage is that UI does not rely on a binning procedure to generate histograms and therefore reduces the statistical error and converges efficiently. We proposed a modified version of WHAM that shares these advantages by representing the biased probability distribution for each window as an analytical normal distribution function rather than the histogram obtained from a binning procedure. The second advantage is that UI can provide accurate PMF curves efficiently even with a small number of windows that do not overlap significantly. In this case, the modified version of WHAM can also provide accurate PMF curves but is more computationally expensive because it requires a large number of iterations for convergence. Thus, UI is a promising method for generating accurate PMF curves for large systems for which sampling may be limited.

Acknowledgments

References

1. Torrie GM, Valleau JP. Chem. Phys. Lett 1974;28:578–581.

2. Ferrenberg AM, Swendsen RH. Phys. Rev. Lett 1988;61:2635–2638. [PubMed: 10039183]

3. Ferrenberg AM, Swendsen RH. Phys. Rev. Lett 1989;63:1195–1198. [PubMed: 10040500]

4. Kumar S, Rosenberg JM, Bouzida D, Swendsen RH, Kollman PA. J. Comput. Chem 1992;13:1011–1021.

5. Roux B. Comput. Phys. Commun 1995;91:275–282.

6. Souaille M, Roux B. Comput. Phys. Commun 2001;135:40–57.

7. Bartels C, Karplus M. J. Comput. Chem 1997;18:1450–1462.

8. Kastner J, Thiel W. J. Chem. Phys 2005;123:144104. [PubMed: 16238371]

9. Kastner J, Thiel W. J. Chem. Phys 2006;124:234106. [PubMed: 16821906]

10. Warshel, A. Computer Modeling of Chemical Reactions in Enzymes and Solutions. John Wiley & Sons, Inc.; New York: 1991.

11. Schmitt UW, Voth GA. J. Phys. Chem. B 1998;102:5547–5551.

12. Vuilleumier R, Borgis D. Chem. Phys. Lett 1998;284:71–77.

13. Cembran A, Gao J. Theor. Chem. Acc 2007;118:211–218.

14. Truhlar DG. J. Comput. Chem 2007;28:73–86. [PubMed: 17058184]

15. Billeter SR, Webb SP, Iordanov T, Agarwal PK, Hammes-Schiffer S. J. Chem. Phys 2001;114:6925–6936.

16. Agarwal PK, Billeter SR, Hammes-Schiffer S. J. Phys. Chem. B 2002;106:3283–3293.

17. Wong KF, Watney JB, Hammes-Schiffer S. J. Phys. Chem. B 2004;108:12231–12241.

18. Wang Q, Hammes-Schiffer S. J. Chem. Phys 2006;125:184102. [PubMed: 17115733]

19. Watney JB, Soudackov AV, Wong KF, Hammes-Schiffer S. Chem. Phys. Lett 2006;418:268–271.

20. Malcolm MA, Simpson RB. ACM Transactions on Mathematical Software 1975;1:129–146.

21. Piessens R, Branders M. Mathematics of Computation 1974;28:135–139.

22. Mathematica. Vol. Version 6.0. Wolfram Research, Inc.; Champaign, IL: 2007.

23. Schiferl SK, Wallace DC. J. Chem. Phys 1985;83:5203–5209.

24. Stuart, A.; Ord, JK. Kendall's Advanced Theory of Statistics. Vol. Sixth. Vol. 1. John Wiley & Sons, Inc.; New York: 1994. p. 228-229.Distribution Theory

25. Blinnikov S, Moessner R. Astronomy & Astrophysics Supplement Series 1998;130:193–205.

26. Sawaya MR, Kraut J. Biochemistry 1997;36:586–603. [PubMed: 9012674]

27. van Gunsteren, WF.; Billeter, SR.; Eising, AA.; Hunenberger, PH.; Kruger, P.; Mark, AE.; Scott, WRP.; Tironi, IG. Biomolecular simulation: The GROMOS96 manual and user guide. VdF Hochschulverlag, ETH Zurich; Zurich: 1996.

28. Fierke CA, Johnson KA, Benkovic SJ. Biochemistry 1987;26:4085–92. [PubMed: 3307916]

29. Kobrak MN. J. Comput. Chem 2003;24:1437–1446. [PubMed: 12868109]
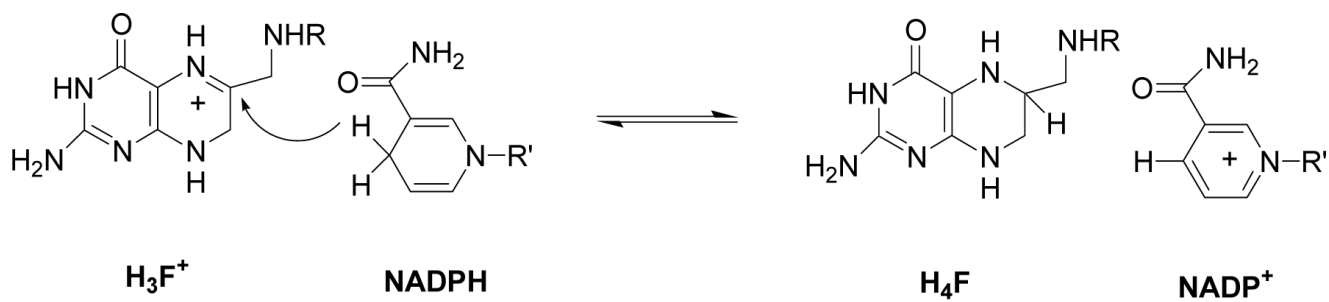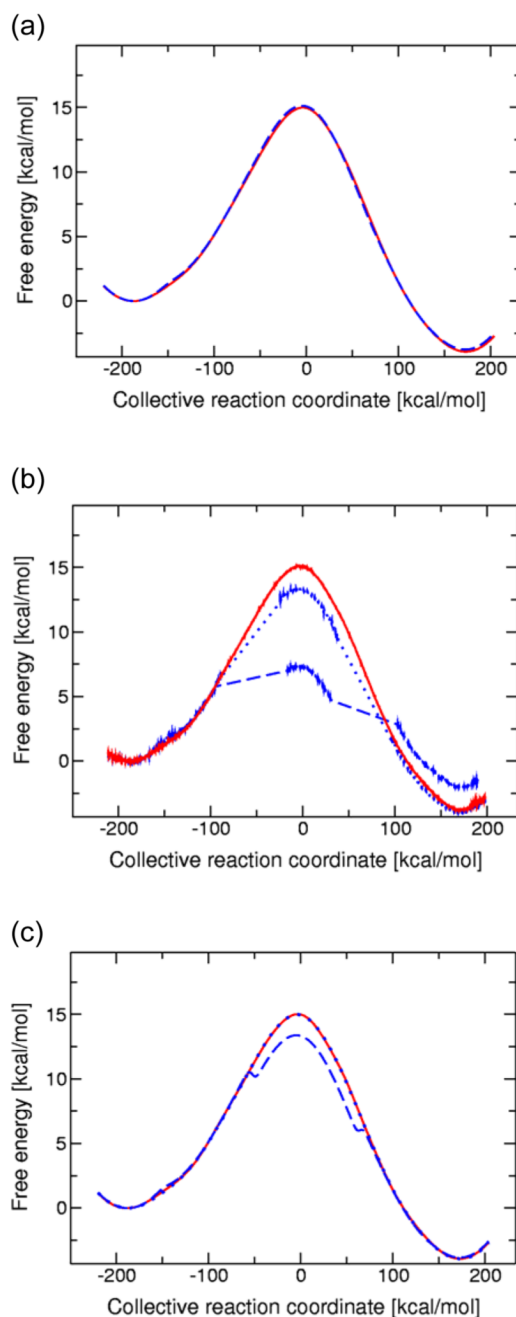
Figure 1.
Hydride transfer reaction from the NADPH cofactor to the protonated dihydrofolate substrate H_3F^+ to form the products tetrahydrofolate H_4F and $NADP^+$.
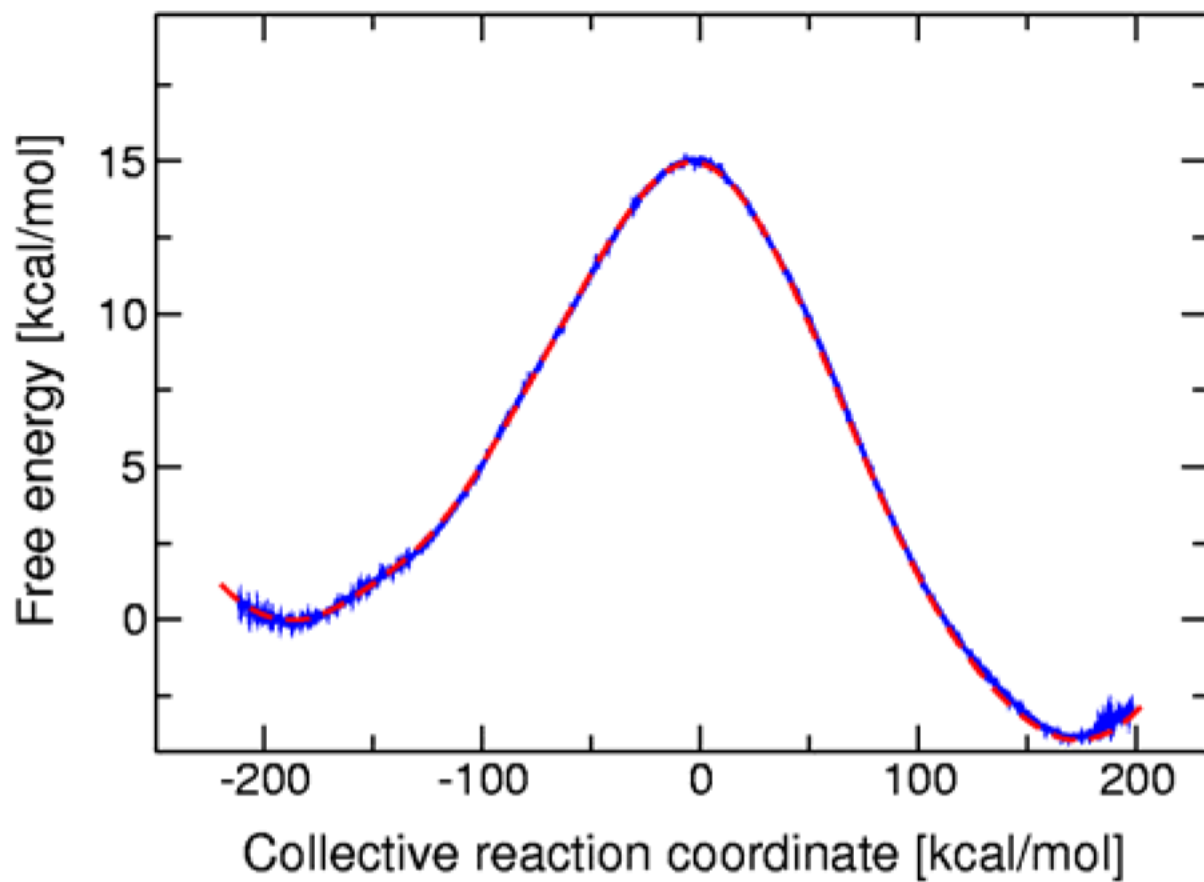
Figure 2.
PMF for the hydride transfer reaction generated with UI (red dashed) and WHAM (blue solid) with a bin size of 1.0 kcal/mol.
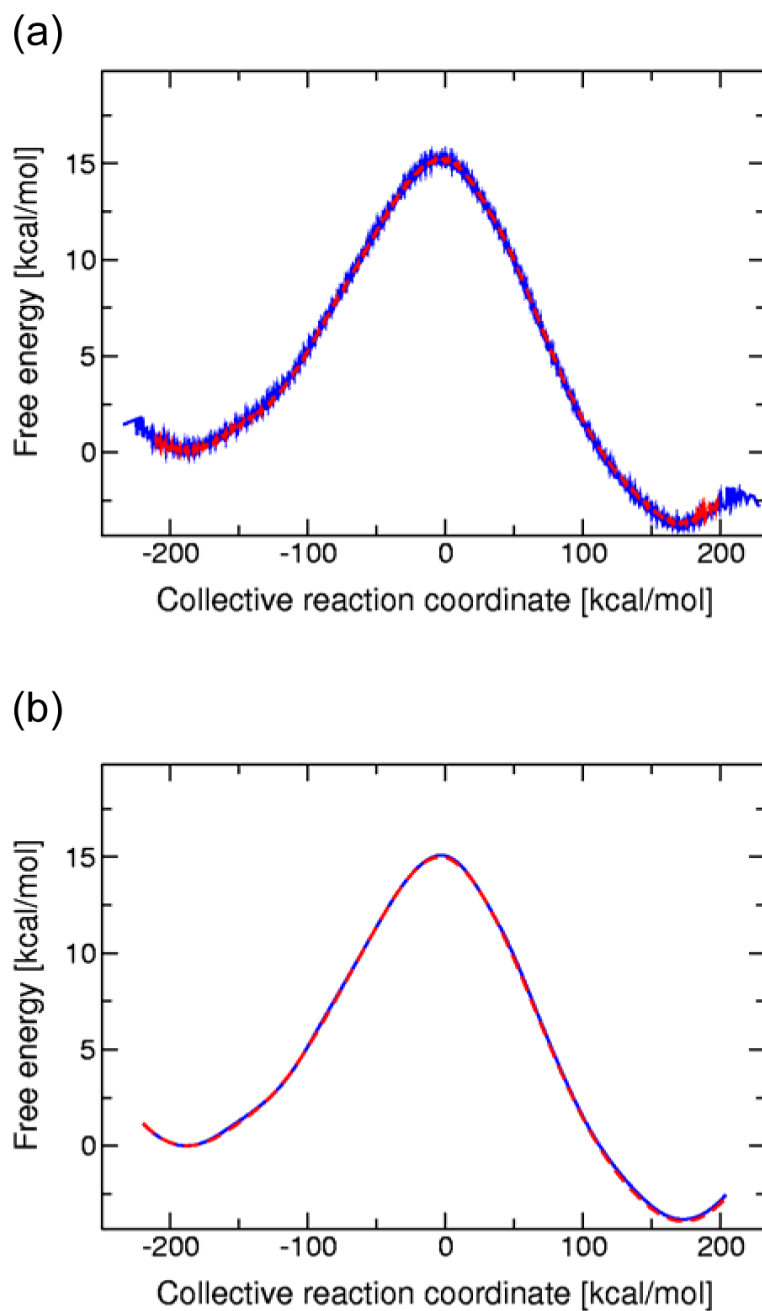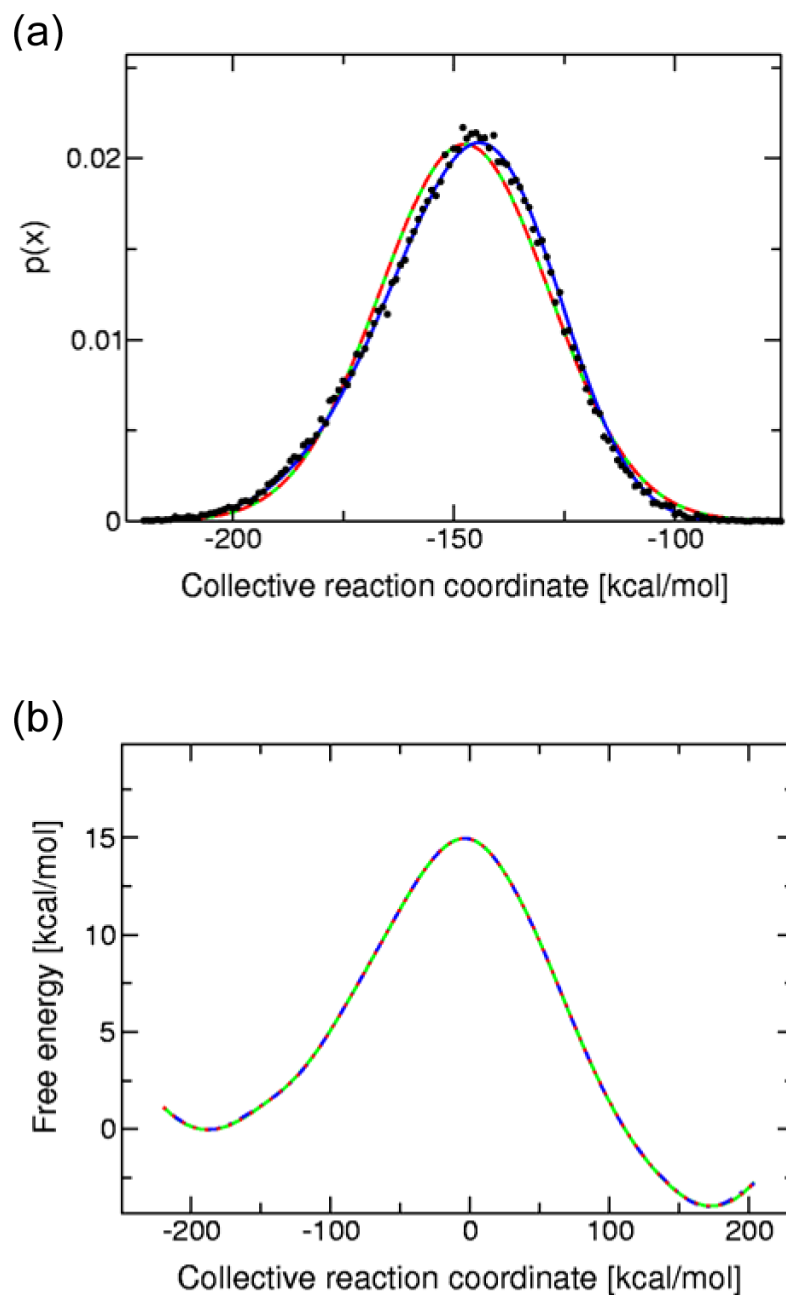
Figure 3.
PMF for the hydride transfer reaction generated with (a) WHAM using a bin size of 1.0 kcal/mol (red dashed) and 0.2 kcal/mol (blue solid) and (b) UI (red dashed) and WHAM(n) (blue solid). The UI and WHAM(n) PMF curves are virtually indistinguishable.

Figure 4.
PMF for the hydride transfer reaction generated using 19 windows (red solid) and five windows (blue dashed or dotted) with (a) UI, (b) WHAM, and (c) WHAM(n). For UI, the two PMF curves are virtually indistinguishable. The PMF curves generated with WHAM are shown for a convergence criterion of 10^{-4} (dashed) and 10^{-8} (dotted). The PMF curves generated with WHAM(n) are shown for a convergence criterion of 10^{-4} (dashed) and 10^{-6} (dotted). The 19 windows correspond to equally spaced values of λ_i in the range $\lambda_i = 0.05$ to 0.95, and the five windows correspond to $\lambda_i = 0.05, 0.15, 0.50, 0.85, 0.95$.

(a)

(b)

Figure 5.
(a) Biased probability distribution function for the window with $\lambda_i = 0.10$, where the filled circles represent the normalized histogram constructed from the simulation data and the solid and dashed lines represent fits to a normal distribution (red), a Gram-Charlier expansion to third order (green), and an Edgeworth expansion with three terms (blue). (b) PMF curves generated with the three fits in (a). The three PMF curves are virtually indistinguishable.